Sensitivity indices based on the *G-Scheme*

Mauro Valorani*, S. Paolucci†, Habib N. Najm‡
* Sapienza, University of Rome, Rome, Italy
† University of Notre Dame Notre Dame, IN,USA
‡ Sandia National Laboratories, Livermore, CA, USA

***Abstract*— A new set of importance indices based on the *G-Scheme* framework are presented. They provide information on the relative importance of selected processes in determining the slow, active, and fast dynamics of individual species/variables. These new indices are scaled measures of the (projected) contribution of each process over the currently driving time scale. This fact allows the introduction of *G-Scheme* sensitivity indices as well as of new importance indices.**

I. Introduction

Lam carried out a CSP-based sensitivity analysis in [1] showing that "the most interesting sensitivity questions [in the analysis of a kinetic system] can be answered by interrogating the CSP data," *i.e.*, participation and importance indices, and pointers to CSP radicals. In addition, he derived an estimate of the response of the kinetic system *in the slow time epoch* as induced by perturbations of the original vector field evaluated along the unperturbed trajectory.

Later, the CSP data were extensively and successfully used in the development of methods to generate simplified kinetic mechanisms, where the opportunity emerged to attribute the adjective "slow" to the original importance index, and at the same time, to introduce a new "fast" importance index [2]. These extended definitions of the indices were instrumental to assess both the relative importance of a specific process (reaction) in the slow dynamics of a major (non-CSP radical) species/variable through the corresponding slow importance index, and in the construction of a slow invariant manifold defining an equation of state for a CSP radical through the corresponding fast importance index.

Recently, we introduced a numerical technique consisting of an algorithmic framework [3], named the *G-Scheme*, to achieve multi-scale adaptive model reduction along-with the integration of the reduced **d**ifferential **e**quations (DEs). The dynamics is decomposed into active, slow, fast, and when applicable, invariant subspaces. The *G-Scheme* introduces a locally curvilinear frame of reference, defined by a set of orthonormal basis vectors with corresponding coordinates, attached to this decomposition. The evolution of the curvilinear coordinates associated with the active subspace is described by non-stiff DEs, whereas those associated with the slow and fast subspaces are accounted for by applying algebraic corrections derived from asymptotics of the original system. Adjusting the number of active DEs dynamically during the time integration is the most significant feature of the *G-Scheme*, since the numerical integration is accomplished by solving a number of DEs typically much smaller than the dimension of the original problem, with corresponding saving in computational work.

Considering that the formulation of the set of ODEs integrated in the *G-Scheme* is obtained by performing a local perturbation of the system dynamics, in the present work we derive a new set of *local* indices, which provide estimates of the error affecting a specific species/variable associated with the removal/modification of a reaction/process contributing to the vector field. Moreover, we introduce sensitivity indices to assess the relative importance of a process to the slow, active, and fast dynamics according to the decomposition of the tangent space defined by the *G-Scheme*. Global information can be deduced by considering the infinity-norm or the time-weighted averages of these indices along selected trajectories.

II. Theory

In the *G-Scheme* framework, a local change of frame of reference, defined by a set of orthonormal basis vectors $\{\boldsymbol{a}_i\}_{i=1}^N$ and their duals $\{\boldsymbol{b}^i\}_{i=1}^N$, is used to decompose the tangent space $\mathcal{T}_{\boldsymbol{x}}$ at $\boldsymbol{x}(t)$ as the direct sum of four basic subspaces[1] $\mathcal{T}_x = \mathbb{E} \oplus \mathbb{H} \oplus \mathbb{A} \oplus \mathbb{T}$. Under this mapping, the time evolution of the state vector $\boldsymbol{x} \in \mathbb{R}^N$ can be obtained as:

$$\begin{aligned} \boldsymbol{x}(t) &= \boldsymbol{x}_n + \Delta\boldsymbol{x}, \\ &= \boldsymbol{x}_n + \Delta\boldsymbol{x}^e + \Delta\boldsymbol{x}^h + \Delta\boldsymbol{x}^a + \Delta\boldsymbol{x}^t, \end{aligned} \quad (1)$$

where $\boldsymbol{x}_n = \boldsymbol{x}(t_n)$ is the state vector at time t_n, and $e = 1, E$, $h = E+1, H-1$, $a = H, T$, and $t = T+1, N$. The contributions of the four subspaces to the perturbation vector $\Delta\boldsymbol{x}$ *over the currently active time scale*[2] τ_T, is estimated, after local linearization, as:

$$\Delta\boldsymbol{x}^h \approx \tau_T\, A_h\, B^h \left(I + \tfrac{1}{2}\Lambda_h^h \tau_T\right) \boldsymbol{f}(\boldsymbol{x}_n), \quad (2)$$

$$\Delta\boldsymbol{x}^a \approx A_a\, B^a \left(\tfrac{e^{\Lambda_a^a \tau_T} - I}{\Lambda_a^a}\right) \boldsymbol{f}(\boldsymbol{x}_n), \quad (3)$$

$$\Delta\boldsymbol{x}^t \approx -A_t\, \left(B^t\, J\, A_t\right)^{-1} B^t\, \boldsymbol{f}(\boldsymbol{x}_n + \Delta\boldsymbol{x}^h + \Delta\boldsymbol{x}^a) \quad (4)$$

for the contribution of the slow, $\mathbb{H}$, active, $\mathbb{A}$, and fast, $\mathbb{T}$, subspaces respectively, where the matrices $A_{h,a,t}$ are formed by the column vectors $\boldsymbol{a}_{h,a,t}$, respectively, the matrices $B^{h,a,t}$ are formed by the row vectors $\boldsymbol{b}^{h,a,t}$, J is the Jacobian matrix of the vector field $\boldsymbol{f}$, and, to leading

[1] The active subspace $\mathbb{A}$ contains all intermediate, currently active (dynamic) time scales. All scales slower/faster than the active ones are confined to the subspaces $\mathbb{H}$/$\mathbb{T}$, and, if the system possesses invariants, $\mathbb{E}$ is the subspace spanned by the directions associated with them.

[2] τ_T is the fastest of the time scales in the active subspace $\mathbb{A}$.

order, $\Lambda_i^i \approx B^i\, J\, A_i$. By construction, the contribution $\Delta \boldsymbol{x}^e$ of the invariant subspace is identically zero.

Eq. (4) provides an estimate of the asymptotic contribution of the fast scales, whose accuracy increases with the magnitude of the gap between the fastest of the active scales, τ_T, and the slowest of the fast scales, τ_{T+1}. In the *G-Scheme*, the contribution of the active scales is obtained by solving a set of nonlinear ODEs with an explicit solver (ERK4).

Now, let us consider the case of a vector field having the structure

$$\boldsymbol{f}(\boldsymbol{x}) = \sum_{k=1}^{\mathfrak{R}} \boldsymbol{f}_k(\boldsymbol{x}) = \sum_{k=1}^{\mathfrak{R}} \boldsymbol{S}_k r^k(\boldsymbol{x}) \tag{5}$$

where $\boldsymbol{S}_k$ and $r^k(\boldsymbol{x})$ are the stoichiometric vector and the (forward/reverse) rate associated with the k-th reaction, $\mathfrak{R} = 2N_r$, and N_r is the number of reversible reactions.

It is worth recalling the definitions of the slow/fast CSP importance indices:

$$\begin{aligned} I_{s,k}^i &= \frac{C_{s,k}^i r^k}{\sum_{k'=1}^{\mathfrak{R}} |C_{s,k'}^i r^{k'}|}, \quad C_{s,k}^i = \sum_s a_s^i (\boldsymbol{b}^s \cdot \boldsymbol{S}_k), \\ I_{r,k}^i &= \frac{C_{r,k}^i r^k}{\sum_{k'=1}^{\mathfrak{R}} |C_{r,k'}^i r^{k'}|}, \quad C_{r,k}^i = \sum_r a_r^i (\boldsymbol{b}^r \cdot \boldsymbol{S}_k). \end{aligned} \tag{6}$$

where s=1,T, and r=T+1,N. These indices measure the (non-dimensional) relative importance of the *instantaneous* contribution of the k-th reaction to the slow/fast dynamics of the i-th species in the projected vector field $P_{s,r}\boldsymbol{f}(\boldsymbol{x}(t))$, with the projector matrices defined as $P_{s,r} = A_{s,r} B^{s,r}$.

Given the linearity of Eqs. (2-4) and (5), the contribution of the k-th reaction reads (no sum on k):

$$\begin{aligned} \Delta \boldsymbol{x}_k^h &\approx \tau_T\, A_h\, B^h \left(I + \frac{1}{2} \Lambda_h^h \tau_T \right) \boldsymbol{S}_k r^k(\boldsymbol{x}_n), \\ \Delta \boldsymbol{x}_k^a &\approx A_a\, B^a \left(\frac{e^{\tau_T \Lambda_a^a} - I}{\Lambda_a^a} \right) \boldsymbol{S}_k r^k(\boldsymbol{x}_n), \\ \Delta \boldsymbol{x}_k^t &\approx -A_t \left(B^t\, J\, A_t \right)^{-1} B^t\, \boldsymbol{S}_k r^k(\boldsymbol{x}_n). \end{aligned} \tag{7}$$

where all coefficients are evaluated at $\boldsymbol{x}_n$. The terms $\Delta \boldsymbol{x}_k^t$ in (7) are evaluated at $\boldsymbol{x}_n$ since these terms are computed during the post-processing of numerical solutions generated by the G-Scheme, whereas $\Delta \boldsymbol{x}^t$ in (4) is evaluated at $\boldsymbol{x}_n + \Delta \boldsymbol{x}^h + \Delta \boldsymbol{x}^a$ since it is used to generate the solution during the numerical integration. The state vector $\boldsymbol{x}_n$ lies by construction on a (N-T)-dimensional SIM, whereas in general $\boldsymbol{x}_n + \Delta \boldsymbol{x}^h + \Delta \boldsymbol{x}^a$ does not. As a consequence the sum of the non-zero terms $\Delta \boldsymbol{x}_k^t$ over all reactions at $\boldsymbol{x}_n$ is approximately zero whereas $\Delta \boldsymbol{x}^t$ in (4) is usually different from zero[3].

The terms $\Delta \boldsymbol{x}_k^{h,a,t}$ in (7) are approximations of the *integral over the driving time scale*, τ_T, of the projection of the k-th reaction over the slow (h), active (a), and fast (t) subspaces, that is:

$$\Delta \boldsymbol{x}_k^{h,a,t} \approx \int_{t_n}^{t_n+\tau_T} P_{h,a,t}\, \boldsymbol{f}_k(\boldsymbol{x}(t)) dt, \tag{8}$$

with the projector matrices now defined as $P_{h,a,t} = A_{h,a,t} B^{h,a,t}$.

The variation Δx_k^i of the i-th species/variable due to the action of the k-th reaction over the three subspaces can be estimated as:

$$\Delta x_k^i = \Delta x_k^{i,h} + \Delta x_k^{i,a} + \Delta x_k^{i,t}. \tag{9}$$

Summing over all reactions, $\sum_{k=1}^{\mathfrak{R}} \Delta x_k^i$, yields a good approximation of the actual state vector change over the time scale τ_T as computed by the *G-Scheme* integration. Thus, we can introduce an error index as:

$$\varepsilon^i := \left| \frac{\sum_{k=1}^{\mathfrak{R}} \Delta x_k^i}{x^i(t_n + \tau_T) - x^i(t_n)} - 1 \right|. \tag{10}$$

which measures the accuracy of the linearizations used to obtain Eqs. (7).

In the same spirit of the CSP indices, we can now introduce the following normalized indices (no sum on k):

$$G_{(h,a,t),k}^i = \frac{\Delta x_k^{i;h,a,t}}{\sum_{k'=1}^{\mathfrak{R}} |\Delta x_{k'}^{i;h,a,t}|}. \tag{11}$$

The indices $G_{(h,a,t),k}^i$ provide a non-dimensional measure of the *integrated* contribution *over the driving time scale*, τ_T, of the k-th reaction to the slow (h), active (a), and fast (t) dynamics of the i-th species/variable. By construction, $\sum_k G_{(h,a,t),k}^i = 1$. The main difference between this set of indices and the CSP-based importance indices (6) is the fact that the former are scaled measures of the (projected) contribution of each process to the change in the state vector over the currently driving scale, whereas the latter are scaled measures of the (projected) contribution of each process to the vector field at one time instant. This circumstance suggests using the estimates (7) to construct sensitivity indices as illustrated in the next section.

A. Sensitivity Indices

Let us now consider the case of applying a perturbation $\delta \boldsymbol{f}_k$ at time t_n to the original vector field $\boldsymbol{f}$ having the structure

$$\boldsymbol{f} + \delta \boldsymbol{f}_k = \sum_{k'=1}^{\mathfrak{R}} \boldsymbol{S}_{k'} r^{k'} + \boldsymbol{S}_k \delta r^k. \tag{12}$$

That is, we perturb only the k-th reaction at time t_n. We now want to estimate the local response of the system, *i.e.* its local sensitivity, to such perturbation.

To leading order, the perturbation on the k-th reaction rate will be felt through Eqs. (7) only as a variation

[3]The specific role of $\Delta \boldsymbol{x}^t$ in (4) consists in forcing the state vector to lie on a (N-T)-dimensional SIM.

$\delta\Delta\boldsymbol{x}_k^{h,a,t}$ of the corresponding $\Delta\boldsymbol{x}_k^{h,a,t}$ as follows (no sum on k):

$$\begin{aligned}\delta\Delta\boldsymbol{x}_k^h &\approx \tau_T\, A_h\, B^h \left(I + \frac{1}{2}\Lambda_h^h\, \tau_T\right) \boldsymbol{S}_k \delta r^k,\\ \delta\Delta\boldsymbol{x}_k^a &\approx A_a\, B^a \left(\frac{e^{\tau_T \Lambda_a^a} - I}{\Lambda_a^a}\right) \boldsymbol{S}_k \delta r^k,\\ \delta\Delta\boldsymbol{x}_k^t &\approx -A_t\, \left(B^t\, J\, A_t\right)^{-1} B^t\, \boldsymbol{S}_k \delta r^k,\end{aligned} \tag{13}$$

where, again, all coefficients are evaluated at $\boldsymbol{x}_n$.

Lam [1] provides an estimate of the response of the kinetic system *in the slow time epoch* τ^T as induced by perturbations $\delta\boldsymbol{f}_k$ of the original vector field $\boldsymbol{f}$ as follows (Eq. (54) of [1]):

$$\delta\eta^m \approx O\left(\sum_{m'=1}^{M} \tau_{m'}^m\, \delta f_k^{m'}\right), \quad m = T+1, \ldots, N, \tag{14}$$

with

$$\delta\eta^m := \boldsymbol{b}^m \cdot \delta\boldsymbol{x}, \quad \text{and} \quad \delta f_k^m := \boldsymbol{b}^m \cdot \delta\boldsymbol{f}_k, \tag{15}$$

where $\delta\eta^m$ is the perturbation of the m-th fast curvilinear coordinate η^m induced by $\delta\boldsymbol{f}_k$, and $\boldsymbol{b}^m$ is the m-th dual (fast) CSP vector. Inspection of Eq. (14) reveals that when the projection of the perturbation $\delta\boldsymbol{f}_k$ is orthogonal or nearly orthogonal to the m-th CSP vectors $\boldsymbol{a}_m$ then $\delta\eta^m \approx 0$, *i.e.*, the system's dynamics are unaltered by this specific perturbation. As far as the order of magnitude of the remaining (active and slow) mode amplitude perturbations, Lam states that they can be similarly estimated (or computed), and leaves to the reader the exercise of deriving the explicit expressions.

The third expression in Eq. (13) is equivalent to Eq. (14), once the estimate $\delta\eta^m$ is mapped back to the perturbation vector[4] $\delta\Delta\boldsymbol{x}$ by inverting the definition (15): $\delta\Delta\boldsymbol{x} = \boldsymbol{a}_m \delta\eta^m$, and considering that in our case $\tau_{m'}^m = \left(B^t\, J\, A_t\right)^{-1}$, for $m, m' = T+1, \ldots, N$. The first two expressions in Eq. (13) are the explicit contributions of the perturbations due to the active and slow modes[5].

If the perturbation of the k-th rate has the form $\alpha^k\, r^k$, then $\delta r^k = (1-\alpha^k) r^k$ in Eq. (13); *e.g.*, if $\alpha^k = 0$, the k-th rate is zeroed out, *i.e.*, $\delta r^k = r^k$.

The variation $\delta\Delta x_k^i$ of the i-th species/variable due to the action of the k-th perturbed rate over the three subspaces is estimated as:

$$\delta\Delta x_k^i = \delta\Delta x_k^{i,h} + \delta\Delta x_k^{i,a} + \delta\Delta x_k^{i,t}. \tag{16}$$

Thus, we introduce the error index

$$\epsilon_k^{i;h,a,t}(t) := \frac{|\delta\Delta x_k^{i,h,a,t}(t)|}{|x^i(t+\tau_T) - x^i(t)|} \tag{17}$$

which measures the contribution at time t of the k-th reaction to the perturbation of the i-th species/variable over the driving time scale and for the slow (h), active (a), fast (t) subspaces, respectively, and

$$\epsilon_k^i(t) := \epsilon_k^{i;h}(t) + \epsilon_k^{i;a}(t) + \epsilon_k^{i;t}(t) \tag{18}$$

for the contribution over all subspaces.

Introducing the parameters $\Psi_k^{h,a,t}$ as

$$\Psi_k^{h,a,t} = \max_{i=1,N} \left\{\frac{1}{T}\int_{t=0}^{T} \epsilon_k^{i;h,a,t}(t)dt\right\}, \tag{19}$$

allows us to rank the reactions from the most (largest $\Psi_k^{h,a,t}$) to the least (smallest $\Psi_k^{h,a,t}$) significant to the overall trajectory, and for the slow (h), active (a), fast (t) subspaces, respectively, whereas

$$\Psi_k = \max_{i=1,N} \left\{\frac{1}{T}\int_{t=0}^{T} \epsilon_k^{i}(t)dt\right\} \tag{20}$$

for the contribution over all subspaces.

Using the estimates Eqs. (13) allows the evaluation of the logarithmic derivatives (local sensitivities) for each subspace as

$$\sigma_k^{h,a,t} := \frac{d\ln(\Delta\boldsymbol{x}^{h,a,t})}{d\ln(r^k)} = \frac{r^k}{\Delta\boldsymbol{x}^{h,a,t}} \frac{\delta\Delta\boldsymbol{x}_k^{h,a,t}}{\delta r^k}, \tag{21}$$

and the overall (due to all time scales) local sensitivities:

$$\sigma_k := \frac{d\ln(\Delta\boldsymbol{x})}{d\ln(r^k)} = \frac{r^k}{\Delta\boldsymbol{x}} \frac{\delta\Delta\boldsymbol{x}_k}{\delta r^k}, \tag{22}$$

where both $\Delta\boldsymbol{x}^{h,a,t}$ and $\Delta\boldsymbol{x}$ are given by the *G-Scheme* reference solution.

B. Projected vs. Unprojected Estimates

An estimate $\Delta\tilde{\boldsymbol{x}}_k$ of the changes in the state vector on the basis of the k-th unprojected contribution $\boldsymbol{f}_k$ of the vector field over the time scale τ is given by:

$$\begin{aligned}\Delta\tilde{\boldsymbol{x}}_k &\approx \int_{t_n}^{t_n+\tau} \boldsymbol{f}_k(\boldsymbol{x}(t))dt \approx \int_{t_n}^{t_n+\tau} \left(\boldsymbol{f}_k\left(\boldsymbol{x}_n\right) + J_{\boldsymbol{x}_n} \Delta\tilde{\boldsymbol{x}}_k\right) dt\\ &\approx \left(\frac{e^{J_{\boldsymbol{x}_n}\tau} - I}{J_{\boldsymbol{x}_n}}\right) \boldsymbol{f}_k\left(\boldsymbol{x}_n\right) \approx \tau\, \left(I + \frac{\tau}{2} J_{\boldsymbol{x}_n}\right) \boldsymbol{f}_k\left(\boldsymbol{x}_n\right).\end{aligned} \tag{23}$$

It is instructive to compare $\Delta\tilde{\boldsymbol{x}}_k$ with the estimate $\Delta\boldsymbol{x}_k$ found after projection of the term $\boldsymbol{f}_k$, Eqs. (7) and (2)-(4), as approximations of the actual value.

The estimate (23) is accurate only for time intervals τ of the order of the smallest scale τ_{min} contained in $J_{\boldsymbol{x}_n}$. Clearly, when $\tau_{min} \ll \tau_T$, Eq. (23) becomes inaccurate on the scale $\tau \approx \tau_T$, whereas Eqs. (2)-(4) become more accurate as the gap between τ_{min} and τ_T increases. Thus, for non-stiff problems Eq. (23) can be used safely, whereas Eqs. (2)-(4) ought to be used in stiff problems.

This conclusion might suggest that a set of (unprojected) indices defined on the basis of the (net) reaction rates as:

$$\omega_k^i = \frac{S_k^i (r_f^k - r_r^k)}{\sum_{k=1}^{\mathfrak{R}} |S_k^i (r_f^k - r_r^k)|}, \tag{24}$$

as in the DRG method [4], can be used safely for non-stiff problems, whereas the (projected) indices defined in (6) or (11) ought to be used in stiff problems.

[4]From Eq. (1), $\delta\boldsymbol{x} = \delta\Delta\boldsymbol{x}$.

[5]The "slow" (head) modes in the *G-Scheme* are equivalent to the "dormant" modes in Lam [1].

III. An Example

To provide a simple illustration of the differences between the approximations of Eq. (2-4) and (23), we resort to two 3-dimensional linear models, constructed so as to have the real, negative eigenvalues $\mathrm{diag}(\Lambda) = \left\{-\epsilon_T^{-1}, -1, -\epsilon_H\right\}$, where $\epsilon_T, \epsilon_H < 1$ represent the gaps between the active/fast, and active/slow subspaces. By construction, the driving time scale is $\tau_T = 1$. We next consider a diagonal system, Model I, defined by choosing a 3×3 identity matrix as the right eigenvector matrix A, and a fully coupled system, Model II, defined by choosing A as

$$A = \begin{pmatrix} -1.5 & 0.1 & -0.3 \\ 3. & 4. & 1. \\ -1. & -0.3 & 0.6 \end{pmatrix} \tag{25}$$

with the dual basis matrix $B = A^{-1}$. The linear model is given by

$$\begin{bmatrix} \delta y \\ \delta w \\ \delta z \end{bmatrix}' = A \begin{pmatrix} -\epsilon_T^{-1} & 0 & 0 \\ 0 & -1 & 0 \\ 0 & 0 & -\epsilon_H \end{pmatrix} B \begin{bmatrix} \delta y - \delta y_{ss} \\ \delta w - \delta w_{ss} \\ \delta z - \delta z_{ss} \end{bmatrix}, \tag{26}$$

with initial conditions $\delta y(0) = \delta y_0$, $\delta w(0) = \delta w_0$, $\delta z(0) = \delta z_0$, and $\delta y_{ss}, \delta w_{ss}, \delta z_{ss}$ the fixed point values approached at large times. For Model I, we set $\delta y_0 = \delta w_0 = \delta z_0 = 1$, and $\delta y_{ss} = 0.1, \delta w_{ss} = 0.2, \delta z_{ss} = 0.3$. For Model II, we set $\delta y_0 = \sum_{j=1}^{3} A_j^1 \eta_0^j, \delta w_0 = \sum_{j=1}^{3} A_j^2 \eta_0^j, \delta z_0 = \sum_{j=1}^{3} A_j^3 \eta_0^j$, with $\eta_0 = (1, 1, 1)$ and $\delta y_{ss} = 0, \delta w_{ss} = 0, \delta z_{ss} = 0$.

These linear models mimic the (dissipative) dynamics of the state vector perturbations due to a perturbation of the vector field at any time t of the original trajectory $\boldsymbol{x}(t)$. Thus, we should verify whether both Eqs. (2-4) and Eq. (23) are able to approximate the value attained by the state vector, starting from the given initial conditions, after a time interval of the order of the active time scale ($O(1)$). To this end, we report in Figs. 1-4, the comparison of the perturbations δy, δw, and δz, computed by Eqs. (2-4) and (23). Note that each symbol corresponds to the state vector obtained using a different integration time step. The accuracy can be assessed by comparing the symbols with the solid lines, which trace the exact solutions. Although many dots are drawn on the figures, the only interesting comparisons refer to the time steps of order of 1, since we expect to evaluate Eqs. (2-4) and (23) for $\tau = \tau_T$ $(= 1)$.

Figs. 1-2 relate to Model I whose dynamics is fully decoupled and each unknown decays with a single time scale: δy with the fast scale $\tau = \epsilon_T$, δw with the active scale $\tau = 1$, and δz with the slow scale $\tau = \epsilon_H^{-1}$. Fig. 1 shows that already for a relatively narrow gap ($\epsilon_T = \epsilon_H = 0.2$), Eqs. (2-4) at $\tau = 1$ provide an accurate approximation of the exact solution, whereas the time step of order 1 is too large for the first order approximation used in Eq. (23). This translates into an error which is the largest for the fastest time scales (δy) and progressively decreases for the slower time scales (δw and δz). In this latter case, increasing the accuracy requires the increase of the order of the polynomial in Eq. (23), or reducing the time step to the order of ϵ_T. The comparison becomes even more favorable for Eqs. (13) for gaps wider than 0.2.

In contrast, narrowing the gaps by taking $\epsilon_T = \epsilon_H = 0.9$, Fig. 2 shows that the accuracy of Eqs. (2-4) is far from satisfactory for δy because at time $\tau = 1$ the (not so) fast process has not reached its asymptotic value. Indeed, when the gap narrows too much, the problem is neither stiff nor multi-scale, and therefore applying the asymptotic corrections (2-4), instead of using the regular perturbations (23) causes large errors.

Figs. 3-4 relate to Model II whose dynamics is fully-coupled and all unknowns decay with all time scales. In the stiff case, Fig. 3, the error incurred at $\tau = 1$ on the fast scale by Eq. (23) affects all the unknowns, whereas, at $\tau = 1$, Eqs. (2-4) provide accurate estimates for all three solution components.

Finally, Fig. 4 shows that in the non-stiff case, using Eq. (2-4), instead of the regular perturbation Eq. (23), causes large errors.

IV. Conclusions

We have presented estimates of the contribution of each process to the change in the state vector over the driving time scale, projected along the *h*, *a*, and *t* directions, in the context of the *G-Scheme*. We used these estimates to define associated importance indices. The main difference between the new set of importance indices based on the *G-Scheme* framework and the CSP-based importance/participation indices is the fact that the former are scaled measures of the (projected) contribution of each process to the change in the state vector over the currently driving scale, whereas the latter are scaled measures of the (projected) contribution of each process to the vector field at one time instant. We used this construction to formulate local sensitivity coefficients. We compared the utility of this approach for estimation of the change in the state vector with an alternate approach that does not make use of projections onto a slow manifold. We illustrated the need for using the present projected approach in the case of a stiff problem, where fast processes are quickly exhausted. On the other hand, the unprojected approach is more appropriate when there is no time scale separation.

Acknowledgments

This work was supported by the Italian Ministry of University and Research (MIUR) and the US Department of Energy, Office of Basic Energy Sciences, SciDAC Computational Chemistry Program. Sandia National Laboratories is a multiprogram laboratory operated by Sandia Corporation, a Lockheed Martin Company, for the United States Department of Energy under contract DE-AC04-94-AL85000. SP acknowledges the support from NSF (Award #0650843). We acknowledge the technical support of Ing. T. Grenga in the development of the work reported herein.

REFERENCES

[1] S.H.Lam, Reduced Chemistry Modeling and Sensitivity Analysis, in: Lecture Notes for Aerothermochemistry for Hypersonic Technology, 1994-1995 Lecture Series Programme, Von Karman Institute for Fluid Dynemics, 1995, p. 3.

[2] M.Valorani, F.Creta, D.A.Goussis, H.N.Najm, J.C.Lee, An automatic procedure for the simplification of chemical kinetics mechanisms based on CSP, Comb. and Flame 146 (Issues 1-2) (2006) 29–51.

[3] M.Valorani, S.Paolucci, The G-Scheme: A framework for multiscale adaptive model reduction, In print on J.Comp.Phys. (2009).

[4] T.Lu, C.K.Law, A directed relation graph method for mechanism reduction, Proc. Comb. Inst. 30 (2005) 1333–1341.

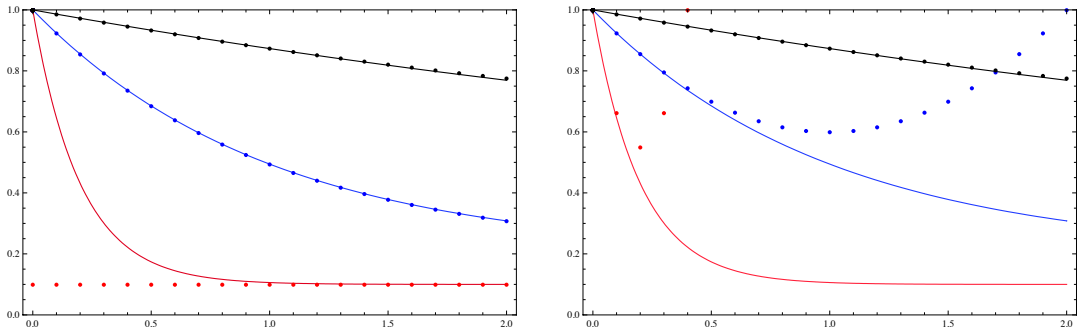

Fig. 1. Model I: $\epsilon_T = \epsilon_H = 0.2$ (stiff) and δy (red), δw (blue), δz (black). Lines are exact and symbols are computed from Eqs. (2)-(4) (left) and Eq. (23) (right).

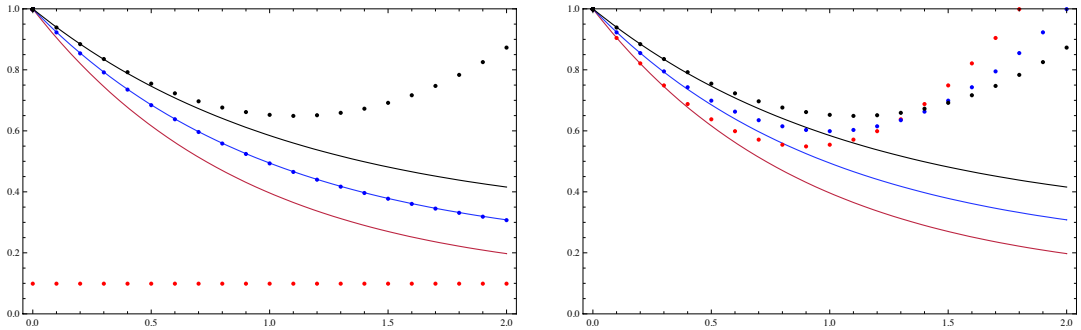

Fig. 2. Model I: $\epsilon_T = \epsilon_H = 0.9$ (non-stiff) and δy (red), δw (blue), δz (black). Lines are exact and symbols are computed from Eqs. (2)-(4) (left) and Eq. (23) (right).

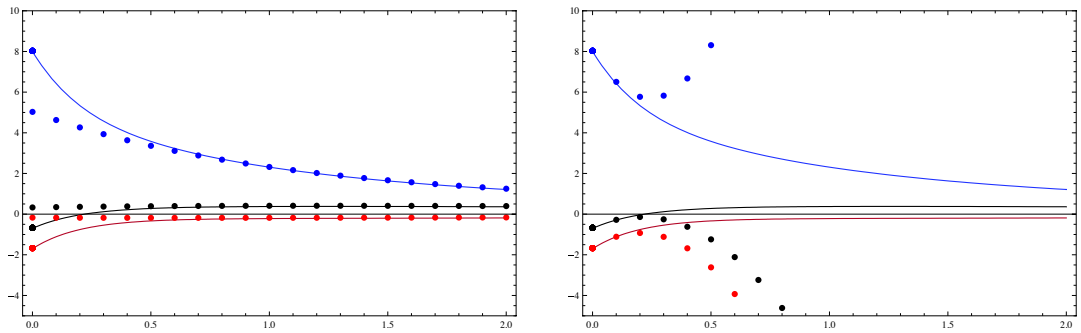

Fig. 3. Model II: $\epsilon_T = \epsilon_H = 0.2$ (stiff) and δy (red), δw (blue), δz (black). Lines are exact and symbols are computed from Eqs. (2)-(4) (left) and Eq. (23) (right).

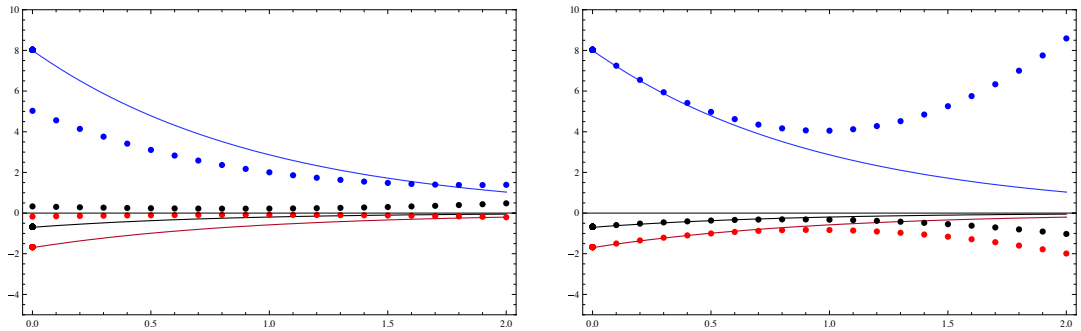

Fig. 4. Model II: $\epsilon_T = \epsilon_H = 0.9$ (non-stiff) and δy (red), δw (blue), δz (black). Lines are exact and symbols are computed from Eqs. (2)-(4) (left) and Eq. (23) (right).